2D Crystallization of Membrane Proteins: Rationales and Examples

Lorenz Hasler,* J. Bernard Heymann,* and Andreas Engel*

Maurice E. Müller Institute for Microscopy, Biozentrum, University of Basel, CH-4056 Basel, Switzerland;

Joerg Kistler†

†*School of Biological Sciences, University of Auckland, New Zealand;*

and

Thomas Walz‡

‡*Krebs Institute for Biomolecular Research, Department of Molecular Biology and Biotechnology, University of Sheffield, United Kingdom*

Received January 5, 1998

The difficulty in crystallizing channel proteins in three dimensions limits the use of X-ray crystallography in solving their structures. In contrast, the amphiphilic character of integral membrane proteins promotes their integration into artificial lipid bilayers. Protein–protein interactions may lead to ordering of the proteins within the lipid bilayer into two-dimensional crystals that are amenable to structural studies by electron crystallography and atomic force microscopy. While reconstitution of membrane proteins with lipids is readily achieved, the mechanisms for crystal formation during or after reconstitution are not well understood. The nature of the detergent and lipid as well as pH and counterions is known to influence the crystal type and quality. Protein–protein interactions may also promote crystal stacking and aggregation of the sheet-like crystals, posing problems in data collection. Although highly promising, the number of well-studied examples is still too small to draw conclusions that would be applicable to any membrane protein of interest. Here we discuss parameters influencing the outcome of two-dimensional crystallization trials using prominent examples of channel protein crystals and highlight areas where further improvements to crystallization protocols can be made. © 1998 Academic Press

[1]Abbreviations used: 2D, 3D, two- and three-dimensional; 8POE, octylpolyoxyethylene; AQP1, aquaporin-1; CMC, critical micellar concentration; DLPC, DL"PC, DMPC, eggPC, dilauryl, dilinoleoyl, dimyristoyl, egg phosphatidylcholine; LPR, lipid:protein ratio; OG, octyl-β-glucoside.

INTRODUCTION

Structure determination of membrane channels is still in its infancy. Classical methods for growing three-dimensional (3D) crystals that have been successfully used to solve the structures of thousands of soluble proteins and protein complexes to atomic resolution by X-ray crystallography are more difficult to apply to membrane proteins. The stumbling block is the considerable hydrophobic surfaces that a channel complex has at its interface with the surrounding lipid. While the channel proteins can be effectively solubilized with detergents that replace the lipid and keep the hydrophobic surfaces of the protein shielded from water, delipidation may destabilize the protein. The use of smaller but harsher detergents may be important for 3D crystallization, as they do not impair protein–protein interactions essential for crystal ordering. The choice of detergent is critical: there is a fine balance between the solubilization of a membrane protein complex in its native conformation and maintaining its structural integrity. A new approach taking advantage of cubic lipidic phases may overcome this major problem, but from initial experiments with bacteriorhodopsin no general conclusion can be drawn yet (see Rummel *et al.,* this issue).

In spite of the difficulties in growing 3D crystals, major progress has recently been made in structure determination of membrane proteins. The archetype family of membrane channels determined to atomic resolution by X-ray diffraction are the porins which form diffusional pores in the outer membrane of mainly Gram-negative bacteria (Cowan *et al.,* 1992; Schirmer *et al.,* 1995, Schirmer, this issue; Weiss and

Schulz, 1992). These pores are 16- or 18-stranded β-barrels with an internal loop contributing to the selectivity properties of the channel. A similar 14-stranded β-barrel fold was found for the transmembrane structure of α-hemolysin, a heptameric toxin from *Staphylococcus aureus* (Gouaux, this issue). The toxin from *Aeromonas hydrophila*, aerolysin, is a soluble protein that forms a heptameric transmembrane channel on cleavage of a C-terminal peptide. The structure of the soluble aerolysin was solved by X-ray crystallography and compared to the membrane-bound structure as determined by electron microscopy (Parker *et al.,* 1994; Rossjohn *et al.,* this issue). The proteolytic removal of the C-terminal peptide on domain 4 exposes a hydrophobic β-sheet surface thought to form part of the channel. In contrast to the β-barrel fold and perhaps a more complex β-sheet fold for aerolysin, the structure of the channel-forming domains of three *Escherichia coli* toxins or colicins (colicins A, E1 and Ia) consists of 10 α-helices thought to rearrange but keep their α-helical character on insertion into the membrane (Elkins *et al.,* 1997; Parker *et al.,* 1992; Wiener *et al.,* 1996). The full-length structure of one of these colicins, colicin Ia, features a 21-nm-long molecule with three distinct domains: the central receptor-binding domain, the N-terminal translocation domain, and the C-terminal channel-forming domain (Wiener *et al.,* 1996).

Although the number of channel structures solved at atomic resolution is small, the knowledge of these structures has significantly improved our understanding of the molecular associations and functions of some important membrane proteins. With such a small number of structures known, it is difficult to ascribe the limited number of folds found (β-barrel or α-helical bundle) to restrictions imposed by the membrane. Thus, it is of paramount importance to determine the structure of many more membrane proteins. As 3D crystallization of membrane proteins proved difficult and slow, alternative approaches to structure determination became essential.

Most importantly, electron crystallography is a structure determination technique that produced excellent results for prokaryotic and eukaryotic membrane proteins (see Walz and Grigorieff, this issue). It has the attractive feature of studying the protein within an environment (the lipid bilayer) close to its natural surroundings. Some channel proteins have a natural propensity to form regular arrays within the native membrane. Most prominently, these include bacteriorhodopsin forming the highly crystalline purple membranes (e.g., Unwin and Henderson, 1975), the acetylcholine receptor channels (Unwin, 1995; Unwin, this issue), and the gap junction channels formed by members of the connexin family (Yaeger *et al.,* this issue).

What to do in cases where a channel of interest occurs only in small numbers, is greatly dispersed in the membrane, and cannot be easily manipulated into crystalline arrays? Most eukaryotic ion channels performing key tasks such as setting the cell resting potentials, conducting action potentials, or regulating cell volume fall into this category. In these cases, where *in situ* crystallization is impossible, 2D crystallization of purified channel proteins offers a workable alternative.

Here, we discuss the three major processes involved in 2D crystallization of membrane channels: (i) reconstitution of the protein into a bilayer; (ii) arrangement or rearrangement of the protein into lattice order, the actual crystallization event; and (iii) crystal folding and clustering. These processes may occur sequentially or concurrently, depending on many poorly understood parameters.

RECONSTITUTION OF MEMBRANE PROTEINS INTO LIPID BILAYERS

To produce high-quality 2D crystals, the protein of interest must usually be purified away from other proteins and contaminants. This involves solubilization of the original membrane with detergent and commonly requires several subsequent separation steps. Finally the pure protein is obtained in a detergent solution, often with residual lipids. The nature of the detergent in both protein purification and subsequent crystallization trials is a critical determinant of success. Most frequently, detergents with a high critical micellar concentration (CMC) such as octyl-β-glucoside (OG) have been used because of the ease with which they can be removed by dialysis. The use of the short-chained phospholipid diheptanoyl phosphatidylcholine as detergent in the purification and crystallization of the photounit of *Rhodospirillum rubrum* (Walz and Ghosh, 1997) is an interesting idea to deal with proteins sensitive to harsh detergents like OG. In fact, phospholipids have already been successfully applied for 3D crystallization experiments (Eisele and Rosenbusch, 1989).

The reconstitution of membrane proteins into bilayers is achieved by decreasing the detergent concentration in the presence of lipids. Figure 1 shows an example where the concentration of octylpolyoxyethylene (8POE) was decreased by dilution and the formation of structures of different sizes was monitored using dynamic light scattering (Dolder *et al.,* 1996). The dilution experiment led to the formation of vesicles with egg phosphatidylcholine (eggPC) or vesicles and 2D crystals with eggPC and the porin OmpF. The gray regions in Fig. 1A indicate distributions of sizes for the two cases. With only lipid
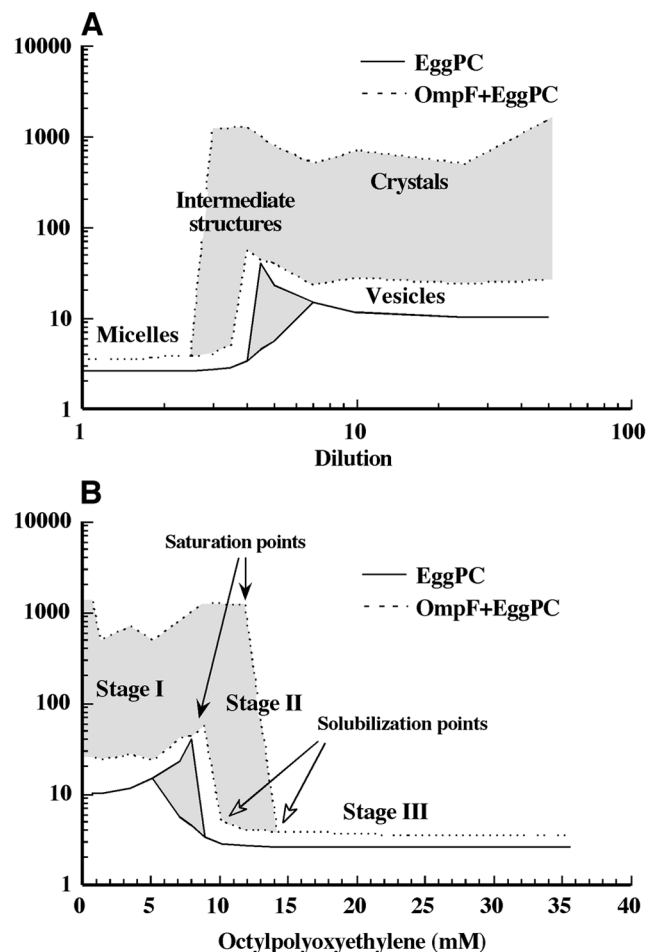
FIG. 1. (A) On dilution of a mixed micellar suspension containing a detergent (octylpolyoxyethylene) and either lipid (eggPC) or lipid and a membrane protein (porin OmpF), at least two populations of structures with different sizes are formed during the transition from micelles to bilayer (the gray areas indicate suspected size ranges). In the case with only eggPC present (continuous line), further dilution results in a homogeneous population of vesicles. With both eggPC and OmpF present (broken line), the two populations are still apparent on further dilution, with the smaller structure vesicles with little incorporated protein and the large structure bilayer with densely packed and crystalline OmpF. (B) The data in A are represented as a function of detergent concentration to illustrate the relationship with the "three-stage" model, with large bilayer structures at low detergent concentrations, small micelles at high concentrations, and a mixture of structures at intermediate concentrations. Data from Dolder *et al.* (1996).

present, the aggregation of mixed lipid-detergent micelles led to a heterogeneous mixture of structures. On further dilution these structures became more homogeneous and finally a single population of vesicles was formed. With both lipid and OmpF present, micellar aggregation started earlier during dilution (Fig. 1A). Again a heterogeneous mixture of structure sizes was observed. However, on further dilution the heterogeneity persisted, leading to the

formation of crystalline tubes and sheets of variable size, as well as vesicles. These vesicles are thought to contain little protein because they were just larger than the vesicles obtained without protein.

A different representation of the same experiment is shown in Fig. 1B to illustrate the relationship between detergent concentration and structure sizes. This representation is commonly used to describe the "three-stage" model of Lichtenberg *et al.* (1983). Stage I is characterized by a detergent concentration that is low enough not to disrupt the lipid bilayer. Stage II is the region of detergent concentration where lipid bilayer and mixed micellar structures coexist. Stage III covers the high detergent concentration where only small micellar structures occur. These specific regions are delineated by the "saturation" and "solubilization" points that define the onset and completion of the solubilization of large structures on addition of detergent.

The micelle-bilayer transition region (Stage II) was found to be the key to reconstitution and by implication to 2D crystallization (Dolder *et al.,* 1996; Engel *et al.,* 1992; Rigaud *et al.,* 1995). Neutron scattering (Hjelm *et al.,* 1992), dynamic light scattering (Egelhaaf and Schurtenberger, 1994), and cryo-electron microscopy (Walter *et al.,* 1991; Egelhaaf, 1995) have shown for several lipid-detergent systems that this transition involves the formation of worm-like extended lipid micelles probably capped by detergents that must convert to vesicles on detergent removal. The abrupt increase in light scattering in the dilution experiment (Fig. 1A) is inferred to arise from the formation of these worm-like structures. Such rod-like structures are therefore thought to be important intermediates in the formation of 2D crystals.

At the start of a typical reconstitution experiment, an excess of detergent ensures a homogeneous distribution of protein and lipid in micelles. As detergent concentration is decreased, lipid and protein interact due to the exposure of their hydrophobic surfaces. With an excess of lipid over protein, the protein is mainly incorporated into lipid bilayers, similar to its native state. In an excess of protein over lipid, the protein mostly ends up in amorphous aggregates, perhaps denatured. Another important parameter is therefore the lipid:protein ratio (LPR), which should be low enough to promote crystal contacts between protein molecules, but not so low that the protein is lost to aggregation.

Reconstitution is closely linked to the properties of the detergents used during both purification and the reconstitution itself (the detergents used for purification can be exchanged for a different detergent used for reconstitution). The manner in which the detergent concentration is decreased is an important

consideration. The commonly used techniques for detergent removal are dilution (Dolder *et al.,* 1996), dialysis (Jap *et al.,* 1992), and selective adsorption of the detergent (Rigaud *et al.,* 1997).

Diluting a solution of protein, lipid, and detergent decreases the concentrations of all components by equal factors, until the free detergent concentration drops below saturation (Fig. 1A). As the protein is significantly diluted during this process, rather high initial concentrations are required. On the other hand, the dilution method allows the process to be arrested when the saturation point is reached, extending the time in which an ordered assembly of the components can take place.

Dialysis is the most widely used technique in 2D crystallization trials, usually in the form of small sample compartments dialyzed against large buffer volumes. To improve the reproducibility of crystallization conditions a temperature-controlled continuous-flow dialysis apparatus was developed (Jap *et al.,* 1992). The major advantage of this system is a precise control of the temperature profile that was found to be quite critical in some cases (Dolder *et al.,* 1993; Ford *et al.,* 1990). Additionally, a maximal gradient of detergent concentration is maintained across the dialysis membrane which improves reproducibility. A drawback of the dialysis method is the long dialysis times needed to remove low CMC detergents, making it only practical for medium to high CMC detergents (typically CMC >1 mM).

The third technique is the selective adsorption of the detergent to hydrophobic substrates or Bio-Beads (Rigaud *et al.,* 1995, 1997). This has been employed with success in the cases of photosystem I complex (Böttcher *et al.,* 1992), cytochrome bc_1 (Akiba *et al.,* 1996), Ca^{2+}-ATPase (Young *et al.,* 1997), the melibiose transporter, and the cytochrome b_6f complex (Rigaud *et al.,* 1997). Because adsorption of lipid together with detergent is undesirable, the Bio-Beads have been thoroughly characterized with radiolabeled detergents and lipids (Lévy *et al.,* 1990). It was found that the adsorption of lipids was significant but very limited, so that minimal removal of lipid is achievable with amounts of beads that remove essentially all detergent. The difficulty in quantitation of the Bio-Beads is perhaps the biggest drawback of this technique.

## PROTEIN REARRANGEMENTS LEADING TO CRYSTALLIZATION

The homogeneity and order of naturally occurring 2D crystals are only rarely sufficient to allow their direct use in structural studies. The prime examples are bacteriorhodopsin in the purple membrane (Grigorieff *et al.,* 1996; Kimura *et al.,* 1997), connexin in gap junctions (Unger *et al.,* 1997), and photosystem

II complexes (Bassi *et al.,* 1989; Lyon *et al.,* 1993). In these cases detergent extraction of native membranes under nonsolubilizing conditions promotes or improves crystallinity. Alternatively, crystallization has been induced by removing excess lipid with phospholipase A_2 as demonstrated with the voltage-dependent anion-selective channel (Mannella, this issue).

When the membrane protein is reconstituted from a mixture of solubilized components, crystal ordering of proteins may occur during reconstitution. In some cases it is difficult to distinguish parameters affecting the incorporation of protein into the lipid bilayer from those leading to crystalline order. In other cases these two processes are quite distinguishable. For crystal packing during reconstitution, the LPR of the reconstitution experiment must be as low as possible to ensure close packing without leading to excessive aggregation. This parameter is quite unpredictable, as was shown in the reconstitution of bacterial cytochrome oxidases, where the optimal LPR for obtaining crystalline order was given as 1.25:1 in one case and as 3:1 in another (Warne *et al.,* 1995). A likely explanation for this discrepancy in optimal LPR might be variable amounts of aggregated protein in the preparation, leading to a decrease in the amount of protein which actually forms crystals. Therefore, it is advisable to determine the fraction of aggregated protein in a given protein batch by, for example, negative stain electron microscopy or analytical ultracentrifugation. Alternatively, it has also been possible to optimize the LPR for reconstitution and then improve crystal packing by mild digestion of excess lipids with phospholipase A_2 (Jap and Li, 1995; Sass *et al.,* 1989; Walian and Jap, 1990).

The lipid mixture used for reconstitution has an influence on the crystallization results. In general, crystallization is more likely to occur when the lipid bilayers are in the fluid phase. Saturated lipids are chemically stable, but their phase transition temperatures are higher than those of unsaturated lipids and they perform poorly in crystallization trials. Native lipids are often ideal in terms of stability and phase temperatures, and they also provide mixtures of head group charges and molecular geometries similar to membranes from which the protein originated. However, the complexity of such preparations may introduce severe disorder precluding crystal formation. Nevertheless, as synthetic lipids, *E. coli* lipids, soybean lecithin, and egg lecithin have all been successfully used for 2D crystallization, no general recommendations can be made on which lipid or lipid mixture is most suitable for any one particular membrane protein.

With respect to LPR and the nature of the lipid it is
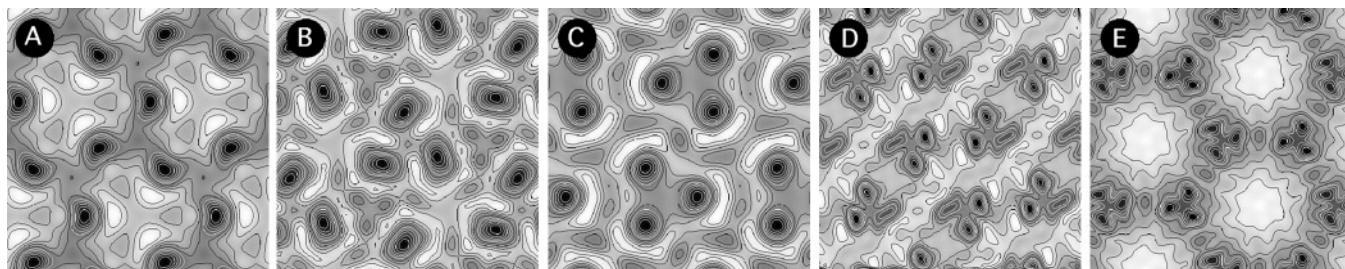
FIG. 2. Porin OmpF exhibits a diversity of crystal forms on reconstitution into lipid bilayers: (A) OmpF reconstituted with DMPC at a LPR = 1.0 gives trigonal lattices with unit cell dimensions $a = b = 9$ nm, which (B) decreases to 7 nm on treatment with phospholipase A_2 (Hoenger *et al.,* 1990). Trigonal lattices with unit cell dimensions $a = b = 8$ nm and rectangular lattices (C) with unit cell dimensions $a = 8$ nm and $b = 13$ nm coexist after reconstitution of OmpF with DMPC at LPR = 0.2. (D) OmpF forms tubular crystals exhibiting a skewed form of the rectangular lattice type when reconstituted in the presence of DL"PC. (E) A trigonal lattice type with unit cell housing two porin trimers and dimensions $a = b = 15$ nm is observed after reconstitution with sphingolipids.

interesting to compare the crystallization behavior of two rather different membrane channels, the β-barrel-forming trimeric bacterial porin OmpF and the α-helical tetrameric human erythrocyte aquaporin AQP1. OmpF assembles into a variety of crystallographic packing arrangements depending on the LPR and the lipid, with unit cells housing one or two porin trimers and unit cell sizes from 7 to 15 nm (Fig. 2). Particularly interesting is the observation that at LPR = 1.0 the chain length of saturated lipids (DMPC and DLPC) as well as the nature of the lipid (the polyunsaturated DL"PC and sphingolipid) had a pronounced effect on unit cell size and morphology (Engel *et al.,* 1992). Although the best-ordered crystals were obtained by lipase A_2 treatment (Sass *et al.,* 1989; Walian and Jap, 1990), different well-ordered crystal forms suggest the possibility of multiple specific interactions, not only between the proteins but also at protein–lipid interfaces.

In contrast to porin OmpF only a single crystallographic packing arrangement was observed with AQP1 (Fig. 3). The best crystals were obtained at LPR = 0.5 which could be related to the lipid:protein ratio found in the crystals themselves (Walz *et al.,* 1994b). At lower LPR the protein started to aggregate, whereas lattices were somewhat less ordered at higher LPR. Virtually identical crystals independent of the lipids used were produced by the dialysis method from OG-solubilized AQP1 from different sources (Fig. 3; Jap and Li, 1995; Mitra *et al.,* 1995; Walz *et al.,* 1995). A subsequent phospholipase A_2 digestion step (Mannella, this issue) increased the amount of well-diffracting 2D crystals in one laboratory, but did not change the lattice parameters significantly (Fig. 3B; Jap and Li, 1995). This indicates that the lipid has little influence on the crystallinity or on the protein packing of AQP1 2D crystals, suggesting a single and dominant set of specific protein–protein interactions between the tetramers. Additionally, AQP1 reconstituted into crystalline
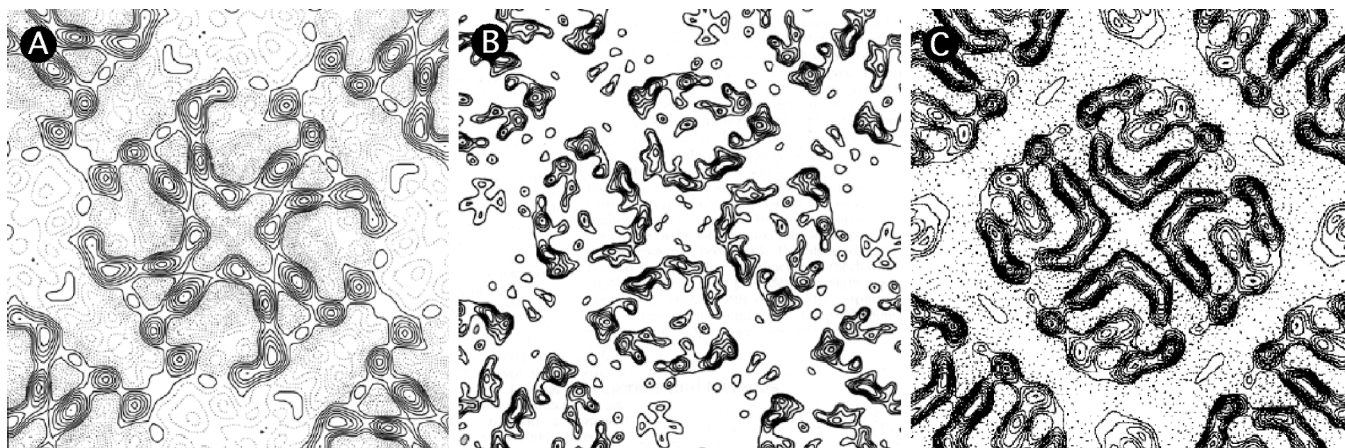
FIG. 3. Crystal packing of AQP1 is independent of the lipid used for reconstitution: AQP1 from human (A and C) or bovine (B) erythrocytes was reconstituted with (A) DOPC at LPR = 1.0 (Mitra *et al.,* 1995), (B) DMPC at LPR = 1.0 (Jap and Li, 1995), and (C) *E. coli* lipids at LPR = 0.5 (Walz *et al.,* 1995). The crystals in B were treated with phospholipase A_2 to remove excess lipids. Projection maps of the unit cells with $p42_12$ symmetry are shown at resolutions of 0.58, 0.35, and 0.6 nm, with unit cell dimensions of $a = b = 10$, 9.64, and 9.6 nm, respectively. Particularly notable is the variation in the density in the center of each monomer between the different maps.

sheets from 4 to 37°C in the presence of *E. coli* lipids at moderately low pH (pH ~6), but crystal order clearly increased with temperature (unpublished data).

Several proteins require a particular ion to produce ordered arrays. Ca^{2+}-ATPase crystallized in the presence of vanadate (Buhle *et al.,* 1983; Young *et al.,* 1997), while the photosystem I reaction center from *Phormidium laminosum* (Ford *et al.,* 1990) and bovine lens connexin (Lampe *et al.,* 1991) required Mg^{2+}. Magnesium was also implicated in the successful crystallization of a porin from *Campylobacter jejuni* (Zhuang *et al.,* 1997). Crystallization of the cytochrome bc_1 complex from a Triton X-100 solution into tubular crystals was found to require the presence of zinc, α-tocopherol, and cardiolipin (Akiba *et al.,* 1996). Optimal conditions for the 2D crystallization of photosystem I from *Synechococcus* included the presence of ammonium ferric citrate, use of the detergent OG, and a particular temperature profile during dialysis (Karrasch *et al.,* 1996). In contrast, AQP1 formed aggregates with ammonium ferric citrate in the dialysis buffer (unpublished data).

The initial detergent concentration and the speed of detergent removal can also be decisive. While dilution from an octyl-β-thioglucoside solution produced tubular crystals of the photosystem II core complex solubilized in dodecyl maltoside, dialysis yielded disordered vesicles loaded with protein, suggesting prolonged exposure to detergent at elevated temperature to be detrimental (Tsiotis *et al.,* 1996). A comprehensive and careful analysis of the parameters influencing the outcome of reconstitution experiments of the microsomal glutathione transferase demonstrated a clear relationship between the initial detergent concentration and the size of the resulting 2D crystals (Schmidt-Krey *et al.,* 1998).

In summary, correct integration of the membrane protein during bilayer formation is a prerequisite for 2D crystallization, but neither the parameters nor the pathways leading to the formation of highly ordered arrays are clear. Specific protein–protein interactions depend on the pH and the presence of specific counterions. To foster protein–protein interactions the LPR needs to be optimized, either during reconstitution or thereafter using phospholipase A_2. Because the micelle–vesicle transition is an abrupt event, it is not clear to what extent crystallization and reconstitution occur simultaneously. The reconstitution temperature is a critical parameter, because the fluidity of the bilayer must allow short- or long-range reordering of the packed proteins. An attractive idea was to use the lipid phase transition to freeze out the proteins, thereby increasing their packing density and promoting crystallization. By cycling between the fluid and gel phases of the lipid,

an improvement of the lattice order was attempted, unfortunately without success (Engel and Hefti, unpublished data). Last but not least, protein–lipid interactions are important. While it is well known that lipids modulate the function of certain membrane proteins, evidence is now accumulating that specific lipids may be required to warrant stability of the solubilized protein during isolation and reconstitution. It is interesting to note that such interactions may also influence the packing arrangement during 2D crystallization (Fig. 2).

CRYSTAL FOLDING AND CLUSTERING

Whenever large 2D crystals are obtained, these thin sheets adopt a variety of shapes, from single layers to stacks and tubes. As a result of protein–protein interactions perpendicular to the plane of the membrane these structures may stick to each other, producing clusters and subsequent problems in obtaining high-quality electron microscopic and atomic force microscopic data.

Depending on the crystallographic packing arrangement and the molecular envelope of the membrane protein, planar and tubular crystal forms emerge. Planar structures are generally found when the packing exhibits a twofold axis or a twofold screw axis in the membrane plane such as with photosystem I (Karrasch *et al.,* 1996), AQP1 (Walz *et al.,* 1997), and LHC II (Kühlbrandt *et al.,* 1994). This is in contrast to arrays in native membranes, such as the purple membranes, which are mostly unidirectional due to the vectorial incorporation of the protein by the cellular machinery. One 2D crystal found in native membranes showing screw axes in the membrane plane is that formed by halorhodopsin overexpressed in *Halobacterium halobium* (Havelka *et al.,* 1993). In this case, a $p42_12$ symmetry was obtained, which may be due to a fraction of incorrectly inserted molecules or fusion of different membranes during isolation.

Folding of planar lattices into tubular forms is the general case for 2D crystals with unidirectional integrated protomers as a result of their intrinsic curvature (Jap *et al.,* 1992). The porin OmpF and maltoporin integrate unidirectionally into membranes on reconstitution to give a mixture of tubes and planar sheets, depending on the conditions. Planar crystals with p3 or p2 symmetry were obtained when OmpF was reconstituted in the presence of DMPC. These crystals occurred either as large vesicles (LPR = 1.0; Fig. 4A) or as doubled-layered sheets (LPR = 0.2; Fig. 4B). Crystallographic packing of the double layers in the latter case (Fig. 4E) is the result of the interactions between the protrusions at the extracellular surface of OmpF (Schabert *et al.,* 1995). Maltoporin forms
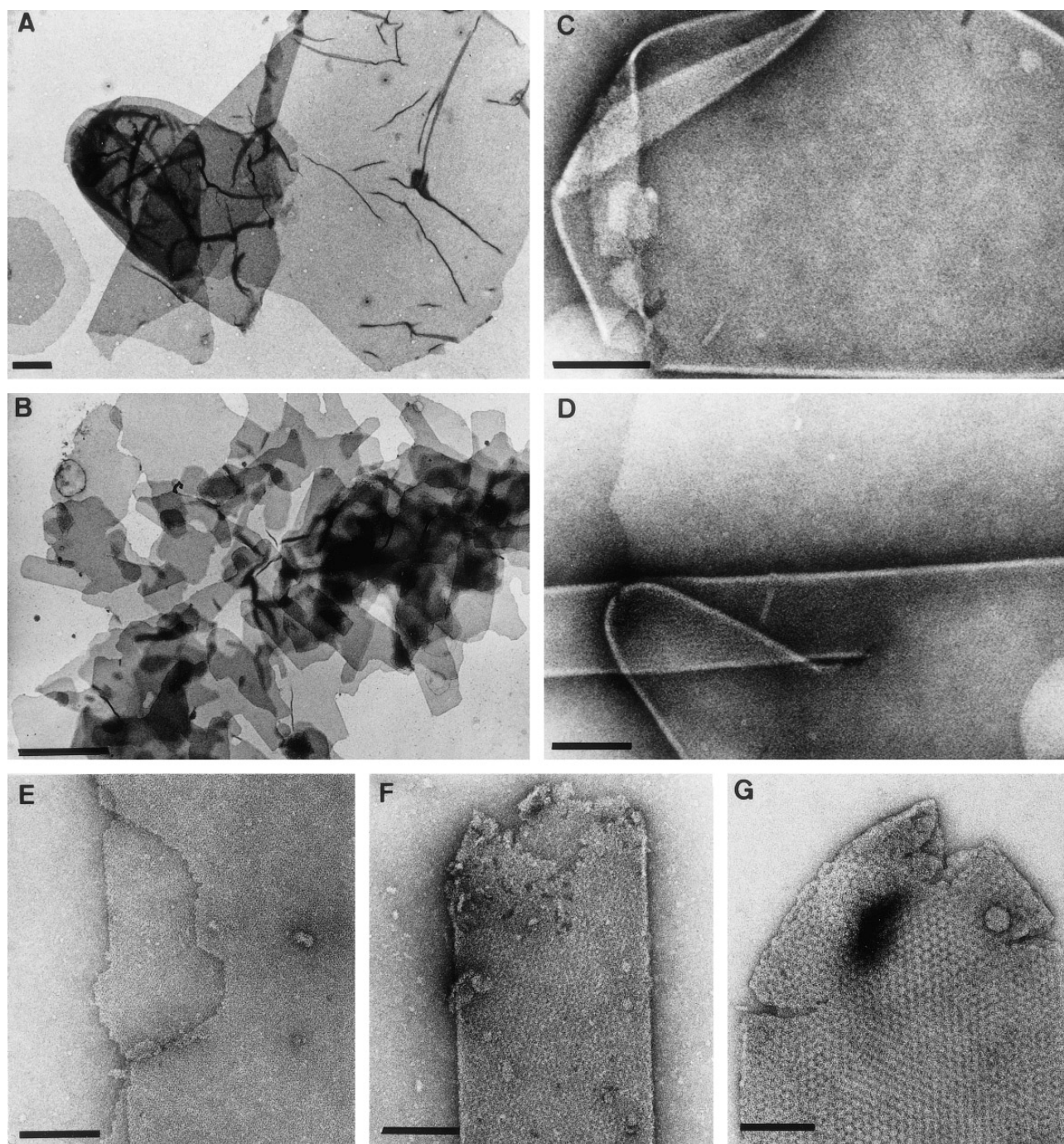
FIG. 4.   Different crystallographic packing arrangements also lead to different large-scale conformations, as illustrated by polymorphic variants obtained on reconstituting porin OmpF and maltoporin into lipid bilayers: 8POE solubilized porin OmpF reconstituted into DMPC gives (A) large folded vesicle-type membranes at LPR = 1.0 and (B) partially overlaid sheet-like structures at LPR = 0.2 (scale bar: 1 µm) (Engel *et al.,* 1992). Maltoporin reconstituted with *E. coli* lipid at LPR = 0.1 yields a mixture of (C) vesicles with double bilayers in flat areas and (D) tubes that occasionally extended into sheets (scale bar: 200 nm) (Stauffer *et al.,* 1992). (E) Porin OmpF trimers reconstituted in DLPC at LPR = 1.0 formed double sheets stacked in register whose order improved after phospholipase A_2 treatment (scale bar: 100 nm) (Engel *et al.,* 1992). (F) Open tubes of rectangular porin OmpF crystals were obtained when reconstituted with DL"PC at LPR = 1.0, while (G) vesicles and capped tubes were obtained with sphingolipids at LPR = 1.0 (scale bar: 100 nm) (Engel *et al.,* 1992).

tubular crystals and vesicles, both flattening into double layers which complicates image processing (Lepault *et al.,* 1988; Stauffer *et al.,* 1992) (Figs. 4C and 4D). OmpF also form tubes in the presence of DL"PC, a polyunsaturated lipid (Fig. 4F), and tubular vesicles with sphingolipids (Fig. 4G).

The amount of counterions may also influence the overall morphology of the crystals, as demonstrated with AQP1 when reconstituted with *E. coli* lipids at pH 6 (Walz *et al.,* 1994a). In several experiments, AQP1 tetramers assembled preferentially into vesicular 2D crystals in the absence of Mg^{2+} and into planar single-layered regular sheets in the presence of Mg^{2+} (Fig. 5). Sheets are preferred because they are often single layered and in general assumed to be better ordered than vesicular crystal forms. The latter, however, are amenable to functional assays developed for noncrystalline proteoliposomes. This allowed the water transport capacity of AQP1 2D crystals to be measured, confirming the native state of AQP1 within the crystalline arrays (Walz *et al.,* 1994b).

ALTERNATIVE METHODS FOR 2D CRYSTALLIZATION

In a few cases the solubilized protein crystallized into sheets or rolls without detergent removal, under conditions similar to those used in 3D crystallization experiments. Bacteriorhodopsin solubilized with Triton X-100 was found to crystallize into orthorhombic lattices when incubated in a solution containing positively charged detergent at pH 4–6 and a temperature of 26–27°C (Michel *et al.,* 1980).

The most significant application of this batch method was for the light-harvesting complex II (LHC-II), which eventually led to atomic resolution (Kühlbrandt and Wang, 1991; Kühlbrandt *et al.,* 1994). As with bacteriorhodopsin, the temperature

profile proved to be critical for the crystallization of LHC-II (Kühlbrandt and Wang, 1991). Recently, Cyrklaff *et al.* (1995) have shown that 2D crystals can also be grown on the surface of a drop from detergent-solubilized and -purified *Neurospora crassa* plasma membrane ATPase. These methods are best interpreted as variations of 3D crystallization and not as proper reconstitution of membrane proteins into a native-like environment.

CONCLUSIONS

Progress with the structure analysis of membrane proteins in general is still limited by difficulties in handling protein–detergent and protein–lipid complexes. This has obstructed the application of traditional structure elucidation methods to membrane proteins, especially X-ray crystallography. The natural tendency of these proteins to integrate into the 2D environment of the lipid bilayer fits perfectly into the application of electron crystallography, provided 2D crystals can be obtained routinely. Alternatively, atomic force microscopy is a suitable tool for determining the surface topography of the native protein complexes and to monitor conformational changes directly in densely packed membranes or 2D crystals (Müller *et al.,* 1997). While the technologies used for collecting and processing electron microscopic data are rapidly improving and are able to provide atomic resolution (Walz and Grigorieff, this issue), the bottleneck remains the crystallization process.

The reconstitution of the membrane protein in the bilayer is without doubt the primary event, but whether crystallization of tightly packed proteins occurs during integration or at a later stage is often not clear. The essential event is the transition from mixed micelle to the bilayer, a step involving a thorough structural rearrangement when the free
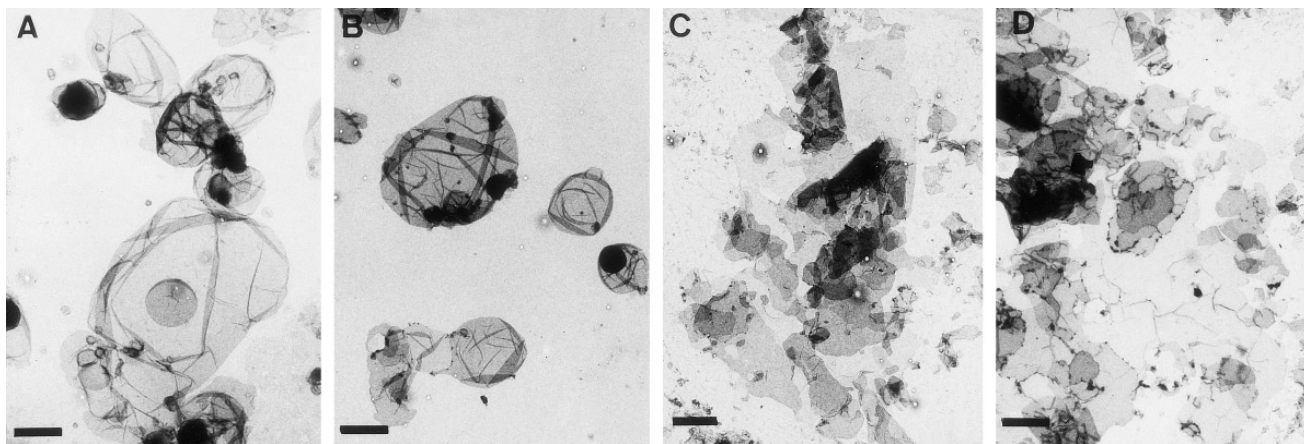
FIG. 5. Reconstitution of AQP1 with *E. coli* lipid at LPR = 0.5 gives predominantly vesicles or sheets, depending on the presence of Mg^{2+} in the dialysis buffer. We observed (A) highly folded crystalline vesicles at 10 mM Mg^{2+}, (B) vesicles and a few small sheets at 20 mM Mg^{2+}, (C) mostly sheets at 40 mM Mg^{2+}, and (D) large 2D crystalline sheets at 50 mM Mg^{2+} (scale bars: 1 μm).

detergent concentration reaches a value close to the CMC. This is probably the most critical process in 2D crystallization irrespective of the detergent removal method and the nature of the constituents. To further improve procedures and to make them more generally applicable, a deeper understanding of the 2D crystallization process is required. This can only be obtained with a systematic analysis of the underlying molecular interactions and events.

REFERENCES

Akiba, T., Toyoshima, C., Matsunaga, T., Kawamoto, M., Kubota, T., Fukuyama, K., Namba, K., and Matsubara, H. (1996) Three-dimensional structure of bovine cytochrome bc_1 complex by electron cryomicroscopy and helical image reconstruction, *Nat. Struct. Biol.* **3,** 553–561.

Bassi, R., Magaldi, A. G., Tognon, G., Giacometti, G. M., and Miller, K. R. (1989) Two-dimensional crystals of the photosystem II reaction center complex from higher plants, *Eur. J. Cell Biol.* **50,** 84–93.

Böttcher, B., Gräber, P., and Boekema, E. J. (1992) The structure of photosystem I from the thermophilic cyanobacterium *Synechococcus* sp. determined by electron microscopy of two-dimensional crystals, *Biochim. Biophys. Acta* **1100,** 125–136.

Buhle, E. L., Knox, B. E., Serpersu, E., and Aebi, U. (1983) The structure of the Ca2+ ATPase as revealed by electron microscopy and image processing of ordered arrays, *J. Ultrastruct. Res.* **85,** 186–203.

Cowan, S. W., Schirmer, T., Rumel, G., Steiert, M., Ghosh, R., Pauptit, R. A., Jansonius, J. N., and Rosenbusch, J. (1992) Crystal structures explain functional properties of two *E. coli* porins, *Nature* **358,** 727–733.

Cyrklaff, M., Auer, M., Kühlbrandt, W., and Scarborough, G. A. (1995) 2-D structure of the *Neurospora crassa* plasma membrane ATPase as determined by electron cryomicroscopy, *EMBO J.* **14,** 1854–1857.

Dolder, M., Engel, A., and Zulauf, M. (1996) The micelle to vesicle transition of lipids and detergents in the presence of a membrane protein: Towards a rationale for 2D crystallization, *FEBS Lett.* **382,** 203–208.

Dolder, M., Walz, T., Hefti, A., and Engel, A. (1993) Human erythrocyte band-3—Solubilization and reconstitution into 2-dimensional crystals, *J. Mol. Biol.* **231,** 119–132.

Egelhaaf, S. U., and Schurtenberger, P. (1994) Shape transformations in the lecithin–bile salt system: From cylinders to vesicles, *J. Phys. Chem.* **98,** 8560–8573.

Egelhaaf, S. U. (1995) A quantitative determination of the structure and size of lecithin-bile salt aggregates in aqueous solution, PhD thesis No. 11366, Swiss Federal Institute of Technology, Zurich.

Eisele, J.-L., and Rosenbusch, J. P. (1989) Crystallization of porin using short chain phospholipids, *J. Mol. Biol.* **206,** 209–212.

Elkins, P., Bunker, A., Cramer, W. A., and Stauffacher, C. V. (1997) A mechanism for toxin insertion into membranes is suggested by the crystal structure of the channel-forming domain of colicin E1, *Structure* **5,** 443–458.

Engel, A., Hoenger, A., Hefti, A., Henn, C., Ford, R. C., Kistler, J., and Zulauf, M. (1992) Assembly of 2-D membrane protein crystals: Dynamics, crystal order, and fidelity of structure analysis by electron microscopy, *J. Struct. Biol.* **109,** 219–234.

Ford, R., Hefti, A., and Engel, A. (1990) Ordered arrays of the photosystem I reaction centre after reconstitution: Projections and surface reliefs of the complex at 2 nm resolution, *EMBO J.* **9,** 3067–3075.

Grigorieff, N., Ceska, T. A., Downing, K. H., Baldwin, J. M., and Henderson, R. (1996) Electron-crystallographic refinement of the structure of bacteriorhodopsin, *J. Mol. Biol.* **259,** 393–421.

Gouaux, E. (1998) α-Hemolysin from *Staphylococcus aureus:* An archetype of β-barrel, channel-forming toxins, *J. Struct. Biol.* **121,** 110–122.

Havelka, W. A., Henderson, R., Heymann, J. A. W., and Oesterhelt, D. (1993) Projection structure of halorhodopsin from *Halobacterium halobium* at 6 Å resolution obtained by electron cryo-microscopy, *J. Mol. Biol.* **234,** 837–846.

Hjelm, R. P., Thiyagarajan, P., and Alkan-Onyuksel, H. (1992) Organization of phosphatidylcholine and bile salt in rodlike mixed micelles, *J. Phys. Chem.* **96,** 8653–8661.

Hoenger, A., Gross, H., Aebi, U., and Engel, A. (1990) Localization of the lipopolysaccharides in metal-shadowed reconstituted lipid–porin membranes, *J. Struct. Biol.* **103,** 185–195.

Jap, B. K., and Li, H. (1995) Structure of the osmo-regulated H_2O-channel, AQP-CHIP, in projection at 3.5 Å resolution, *J. Mol. Biol.* **251,** 413–420.

Jap, B. K., Zulauf, M., Scheybani, T., Hefti, A., Baumeister, W., Aebi, U., and Engel, A. (1992) 2D crystallization: From art to science, *Ultramicroscopy* **46,** 45–84.

Karrasch, S., Typke, D., Walz, T., Miller, M., Tsiotis, G., and Engel, A. (1996) Highly ordered two-dimensional crystals of photosystem I reaction center from *Synechococcus* sp.: Functional and structural analyses, *J. Mol. Biol.* **262,** 336–348.

Kimura, Y., Vassylyev, D. G., Miyazawa, A., Kidera, A., Matsushima, M., Mitsuoka, K., Murata, K., Hirai, T., and Fujiyoshi, Y. (1997) Surface of bacteriorhodopsin revealed by high-resolution electron crystallography, *Nature* **389,** 206–211.

Kühlbrandt, W., and Wang, D. N. (1991) Three-dimensional structure of plant light-harvesting complex determined by electron crystallography, *Nature* **350,** 130–134.

Kühlbrandt, W., Wang, D. N., and Fujiyoshi, Y. (1994) Atomic model of plant light-harvesting complex by electron crystallography, *Nature* **367,** 614–621.

Lampe, P. D., Kistler, J., Hefti, A., Bond, J., Müller, S., Johnson, R. G., and Engel, A. (1991) *In vitro* assembly of gap junctions, *J. Struct. Biol.* **107,** 281–290.

Lepault, J., Dargent, B., Tichelaar, W., Rosenbush, J. P., Leonard, K., and Pattus, F. (1988) Three-dimensional reconstruction of maltoporin from electron microscopy and image processing, *EMBO J.* **7,** 261–268.

Lévy, D., Bluzat, A., Seigneuret, M., and Rigaud, J.-L. (1990) A systematic study of liposome and proteoliposome reconstitution involving Bio-Bead-mediated Triton X-100 removal, *Biochim. Biophys. Acta* **1025,** 179–190.

Lichtenberg, D., Robson, R. J., and Dennis, E. A. (1983) Solubilization of phospholipids by detergents. Structural and kinetic aspects, *Biochim. Biophys. Acta* **737,** 285–304.

Lyon, M. K., Marr, K. M., and Furcinitti, P. S. (1993) Formation and characterization of two-dimensional crystals of photosystem II, *J. Struct. Biol.* **110,** 133–140.

Mannella, C. A. (1998) Conformational changes in the mitochon-

drial channel protein, VDAC, and their functional implications, *J. Struct. Biol.* **121,** 207–218.

Michel, H., Oesterhelt, D., and Henderson, R. (1980) Orthorhombic two-dimensional crystal form of purple membrane, *Proc. Natl. Acad. Sci. USA* **77,** 338–342.

Mitra, A. K., van Hoek, A. N., Wiener, M. C., Verkman, A. S., and Yeager, M. (1995) The CHIP28 water channel visualized in ice by electron crystallography, *Nat. Struct. Biol.* **2,** 726–729.

Müller, D. J., Schoenenberger, C.-A., Schabert, F., and Engel, A. (1997) Structural changes in native membrane proteins at subnanometer resolution with the atomic force microscope: A review, *J. Struct. Biol.* **119,** 149–157.

Parker, M. W., Buckley, J. T., Postma, J. P. M., Tucker, A. D., Leonard, K., Pattus, F., and Tsernoglou, D. (1994) Structure of the *Aeromonas* toxin proaerolysin in its water-soluble and membrane-channel states, *Nature* **367,** 292–295.

Parker, M. W., Postma, J. P. M., Pattus, F., Tucker, A. D., and Tsernoglou, D. (1992) Refined structure of the pore-forming domain of colicin A at 2.4 Å resolution, *J. Mol. Biol.* **224,** 639–657.

Rigaud, J.-L., Mosser, G., Lacapere, J.-J., Olofsson, A., Levy, D., and Ranck, J.-L. (1997) Bio-Beads: An efficient strategy for two-dimensional crystallization of membrane proteins, *J. Struct. Biol.* **118,** 226–235.

Rigaud, J.-L., Pitard, B., and Levy, D. (1995) Reconstitution of membrane proteins in liposomes: Application to energy-transducing membrane proteins, *Biochim. Biophys. Acta* **1231,** 223–246.

Rossjohn, J., Feil, S. C., McKinstry, W. J., Tsernoglou, D., Van Der Goot, G., Buckley, J. T., and Parker, M. W. (1998) Aerolysin—A paradigm for membrane insertion of beta-sheet protein toxins? *J. Struct. Biol.* **121,** 92–100.

Rummel, G., Hardmeyer, A., Widmer, C., Chiu, M. L., Nollert, P., Locher, K. P., Pedruzzi, I., Landau, E. M., and Rosenbusch, J. P. (1998) Lipidic cubic phases: New matrices for the three-dimensional crystallization of membrane proteins, *J. Struct. Biol.* **121,** 82–91.

Sass, H. J., Beckmann, E., Zemlin, F., van Heel, M., Zeitler, E., Rosenbusch, J. P., Dorset, D. L., and Massalski, A. (1989) Densely packed β-structure at the protein–lipid interface of porin is revealed by high-resolution cryo-electron microscopy, *J. Mol. Biol.* **209,** 171–175.

Schabert, F. A., Henn, C., and Engel, A. (1995) Native *Escherichia coli* OmpF porin surfaces probed by atomic force microscopy, *Science* **268,** 92–94.

Schirmer, T. (1998) General and specific porins from bacterial outer membranes, *J. Struct. Biol.* **121,** 101–109.

Schirmer, T., Keller, T., Wamg, Y.-F., and Rosenbusch, J. P. (1995) Structural basis for sugar translocation through maltoporin channels at 3.1 Å resolution, *Science* **267,** 512–514.

Schmidt-Krey, I., Lundqvist, G., Morgenstern, R., and Hebert, H. (1998) Parameters for the two-dimensional crystallization of the membrane protein microsomal glutathione transferase, in preparation.

Stauffer, K. A., Hoenger, A., and Engel, A. (1992) Two-dimensional crystals of *Escherichia coli* maltoporin and their interaction with the maltose-binding protein, *J. Mol. Biol.* **223,** 1155–1165.

Tsiotis, G., Walz, T., Spyridaki, A., Lustig, A., Engel, A., and Ghanotakis, D. (1996) Tubular crystals of a photosystem II core complex, *J. Mol. Biol.* **259,** 241–248.

Unger, V. M., Kumar, N. M., Gilula, N. B., and Yeager, M. (1997) Projection structure of a gap junction membrane channel at 7 Å resolution, *Nat. Struct. Biol.* **4,** 39–43.

Unwin, N. (1998) The nicotinic acetylcholine receptor of the *Torpedo* electric ray, *J. Struct. Biol.* **121,** 181–190.

Unwin, N. (1995) Acetylcholine receptor channel imaged in the open state, *Nature* **373,** 37–43.

Unwin, P. N. T., and Henderson, R. (1975) Molecular structure determination by electron microscopy of unstained crystalline specimens, *J. Mol. Biol.* **94,** 425–440.

Walian, P. J., and Jap, B. K. (1990) Three-dimensional electron diffraction of PhoE porin to 2.8 Å resolution, *J. Mol. Biol.* **215,** 429–438.

Walter, A., Vinson, P., Kaplun, A., and Talmon, Y. (1991) Intermediate structures in the cholate-phosphatidylcholine vesicle–micelle transition, *Biophys. J.* **60,** 1315–1325.

Walz, T., and Ghosh, R. (1997) Two-dimensional crystallization of the light-harvesting I-reaction centre photounit from *Rhodospirillum rubrum*, *J. Mol. Biol.* **265,** 107–111.

Walz, T., and Grigorieff, N. (1998) Electron crystallography of two-dimensional crystals of membrane proteins, *J. Struct. Biol.* **121,** 142–161.

Walz, T., Hirai, T., Murata, K., Heymann, J. B., Mitsuoka, K., Fujiyoshi, Y., Smith, B. L., Agre, P., and Engel, A. (1997) The 6Å three-dimensional structure of aquaporin-1, *Nature* **387,** 624–627.

Walz, T., Smith, B., Agre, P., and Engel, A. (1994a) The three-dimensional structure of human erythrocyte aquaporin CHIP, *EMBO J.* **13,** 2985–2993.

Walz, T., Smith, B., Zeidel, M., Engel, A., and Agre, P. (1994b) Biologically active two-dimensional crystals of aquaporin CHIP, *J. Biol. Chem.* **269,** 1583–1586.

Walz, T., Typke, D., Smith, B. L., Agre, P., and Engel, A. (1995) Projection map of aquaporin-1 determined by electron crystallography, *Nat. Struct. Biol.* **2,** 730–732.

Warne, A., Wang, D. N., and Saraste, M. (1995) Purification and two-dimensional crystallization of bacterial cytochrome oxidases, *Eur. J. Biochem.* **234,** 443–451.

Weiss, M. S., and Schulz, G. E. (1992) Structure of porin refined at 1.8 Å resolution, *J. Mol. Biol.* **227,** 493–509.

Wiener, M. C., Freymann, D. M., Ghosh, P., Finer-Moore, J., and Stroud, R. M. (1996) Progress towards the X-ray crystal structure of colicin Ia, *Biophys. J.* **70,** A140.

Yeager, M. (1998) Structure of cardiac gap junction intercellular channels, *J. Struct. Biol.* **121,** 231–245.

Young, H. S., Rigaud, J.-L., Lacapére, J.-J., Reddy, L. G., and Stokes, D. L. (1997) How to make tubular crystals by reconstitution of detergent-solubilized Ca^{2+}-ATPase, *Biophys. J.* **72,** 2545–2558.

Zhuang, J., Engel, A., Pagès, J.-M., and Bolla, J.-M. (1997) The *Campylobacter jejuni* porin trimers pack into different lattice types when reconstituted in the presence of lipid, *Eur. J. Biochem.* **244,** 575–579.